

Self-Assembly of *n*-Alkanethiols: A Kinetic Study by Second Harmonic Generation

O. Dannenberger,[†] M. Buck,* and M. Grunze

Lehrstuhl für Angewandte Physikalische Chemie, Universität Heidelberg, Im Neuenheimer Feld 253, 69120 Heidelberg, Germany

Received: August 20, 1998; In Final Form: December 10, 1998

Thiolate formation of *n*-alkanethiols ($\text{CH}_3(\text{CH}_2)_{m-1}\text{SH}$) adsorbing on polycrystalline gold was studied in situ and in real time under a variety of experimental conditions. The chain length of the thiols studied varied from $m = 4$ to $m = 22$. The influence of the thiol concentration in different solvents (ethanol, hexane, dodecane, and hexadecane) was examined in the range between 0.5 and 20.0 $\mu\text{mol/L}$. Among the models proposed in the literature, only Langmuir kinetics can explain the data, irrespective of the experimental conditions. As will be shown, all other kinetic models fail to describe the measured formation kinetics of thiolate films on a polycrystalline gold surface. However, small but significant differences between the experimental data and the Langmuir model assuming statistical adsorption are identified. A modified Kisliuk model accounting for different adsorption sites yields the best agreement with the experimental data. On the basis of these results we propose a kinetic model of thiolate formation which identifies the displacement of solvent molecules adsorbed on the substrate and/or incorporation of alkanethiols into thiolate islands as the rate-limiting steps.

1. Introduction

Immersion of a gold substrate in a dilute solution of alkanethiols or dialkyl disulfides leads to the formation of well-ordered self-assembled monolayers (SAMs).^{1–7} These SAMs not only provide excellent model systems to study fundamental aspects of wetting⁸ and tribology,⁹ but also, they are promising candidates for potential applications in the fields of biosensors,^{10,11} biomimetics,¹² and corrosion inhibition.¹³ As shown by a variety of analytical techniques such as infrared spectroscopy,^{4,14} scanning tunneling microscopy (STM),^{15–17} He atom scattering (HAS),¹⁸ grazing incidence X-ray diffraction (GIXD),¹⁹ sum frequency generation (SFG),²⁰ metastable induced electron spectroscopy (MIES),²¹ atomic force microscopy (AFM),²² and near edge X-ray absorption fine structure spectroscopy (NEXAFS),²³ alkanethiolate SAMs are densely packed films. The general understanding is that the molecules are attached to the surface via a gold–thiolate bond, although recent results indicated the possibility that disulfides form.¹⁹ The alkyl chains in the completed monolayer are tilted by an angle of 30°–39° with respect to the surface normal^{4,25} in an all-trans conformation maximizing the interaction energy between the hydrocarbon chains.

Whereas the lateral density and the molecular orientation of the alkyl chains in completed SAMs is known and not controversial, a variety of contradictory publications exists concerning the formation kinetics and the adsorption mechanism from solution.^{2,23,24,26,27,30–39}

The first kinetics experiments were carried out by Bain et al.² who adsorbed octadecanethiol ($\text{CH}_3(\text{CH}_2)_{17}\text{SH}$, C_{18}SH) from ethanol solution with concentrations ranging from 0.1 to 1000 $\mu\text{mol/L}$. Using ellipsometry they found two distinct adsorption steps. The first step in which more than 80% of a monolayer (ML) is formed is completed within minutes. The second step

extends over several hours and is almost independent from the concentration. Films with a thickness of one monolayer can be formed in a variety of different solvents.

The first more quantitative kinetic study of thiol adsorption from solution was done by us using second harmonic generation (SHG). This in situ investigation found the first adsorption step being consistent with a Langmuir adsorption model.^{27,28} In a subsequent ex situ study using NEXAFS the slow, second step could be identified as an ordering process where the alkyl chains initially containing gauche defects are gradually straightened and assume a predominantly all-trans conformation.²³ After immersion of the gold substrates into air-saturated ethanolic solutions of C_{18}SH with concentration of 1000 $\mu\text{mol/L}$ for 6 days, Kim et al. detected the formation of multilayers using scanning tunneling microscopy and a quartz crystal microbalance (QCM).²⁹ Multilayer formation was attributed to the low solubility of oxidized sulfur species in the air-saturated ethanol. Ex situ measurements using a combination of X-ray photoelectron spectroscopy (XPS) and ellipsometry³⁰ as well as Fourier transform infrared reflection absorption spectroscopy (FT-IRRAS) studies²⁴ confirmed the two-step mechanism, first observed by Bain et al.²

Besides these mainly ex situ investigations, there have been a variety of in situ kinetics measurements from different solvents with conflicting results. Shimazu et al. were the first to use an electrochemical quartz crystal microbalance (EQCM) to follow the adsorption of ferrocenylundecanethiol from hexane to gold surfaces in situ.³¹ They also found two subsequent adsorption steps for a concentration of 500 $\mu\text{mol/L}$ with the first step to be completed after formation of only 0.5 monolayer. The second step proceeded slower by 2 orders of magnitude and completion required more than 450 s at a concentration of ca. 1500 $\mu\text{mol/L}$. Since these first in situ (E)QCM measurements, several other studies in different solvents and for a variety of alkanethiols have been conducted. In a comparative study of the adsorption of C_{18}SH from hexane and ethanol, a two-step process was reported for concentrations as high as 1000 and 5000 $\mu\text{mol/L}$.³⁵

* To whom correspondence should be addressed: E-mail: cv6@ix.urz.uni-heidelberg.de.

[†] Current address: Department of Bioengineering, University of Washington, Seattle, WA 98195.

which was proven independently for the adsorption from ethanol for lower concentrations.³⁶ Formation of multilayers in acetonitrile³² and of layers with 20% higher coverage than a monolayer in ethanol³³ was reported. Contrary to the studies summarized above, the QCM measurements of Karpovich et al.³⁴ did not identify a second step in the formation of SAMs of C₈SH or C₁₈SH adsorbed from hexane and/or cyclohexane for concentrations varying from 10 to 1000 $\mu\text{mol/L}$. They suggested the existence of an adsorption/desorption equilibrium resulting in a submonolayer coverage at concentrations of 100 $\mu\text{mol/L}$ and below.

Recently, surface plasmon resonance (SPR) spectroscopy was applied to study film formation kinetics in situ. DeBono et al.³⁷ reported a two step mechanism at concentrations ranging from 10 to 100 $\mu\text{mol/L}$. Whereas the first step gave 50%–80% of a monolayer, the second proceeded 100-fold more slowly and led to thicknesses exceeding one monolayer. Peterlinz and Georgiadis,³⁸ on the other hand, could fit their SPR data with up to three distinct kinetic steps when adsorbing alkanethiols of different chain lengths from ethanol. When varying the concentration from 1 to 1000 $\mu\text{mol/L}$, a 2-fold increase in the adsorption kinetics for the first step could be detected. Their data, contrary to most other results, could not be described by a first-order Langmuir model. They explained their experiments by the existence of a layer of physisorbed thiols on top of a layer of thiolates.

Finally, in the most recent ex situ FT-IRRAS kinetics study, Bensebaa et al.³⁹ presented data from which they concluded immersion times of 45 s are sufficient to form an ordered monolayer of alkanethiols on polycrystalline gold substrates from micromolar solutions.

As is obvious from this short overview, numerous contradictory results have been reported. Therefore, we have carried out detailed quantitative in situ kinetic studies for the adsorption of alkanethiols onto polycrystalline gold with the aim to improve the understanding of film formation. The experiments reported below, however, only consider the first step of film formation which proceeds on a time scale short relative to the subsequent slower step(s) leading to full monolayer coverage. Monitoring the second harmonic signal which detects the chemisorption of the thiol onto the gold surface, thiol adsorption was followed in real time and the influence of essential parameters such as thiol concentration, solvent, and molecular size on the kinetics of film formation was investigated. Comparison of the experimental data with different kinetic models yields best agreement with a model which includes two different pathways of thiolate formation. Different mechanisms and molecular processes on the molecular scale which can, in principle, be rate limiting are discussed with respect to the compatibility with the SHG data.

2. Experimental Section

The experimental setup is shown schematically in Figure 1. A Nd:YAG laser with a fundamental wavelength of $\lambda = 1064$ nm, a pulse duration of 7 ns, and a repetition rate of 10 Hz was used. The beam impinging onto the substrate had a diameter of 2.5 mm, and the energy of the laser pulses incident on the sample was about 2.5 mJ. Thus the light intensity remained far below the damage threshold of the surface which is above 500 mJ/cm².⁴⁰ A color filter was placed between the polarizer and the sample to block unwanted fluorescence and SHG background from the optics. The frequency-doubled light of $\lambda = 532$ nm generated in reflection at the gold surface passed a filter to block the fundamental radiation, a polarizer, and a monochromator with a photomultiplier. The signal was collected by

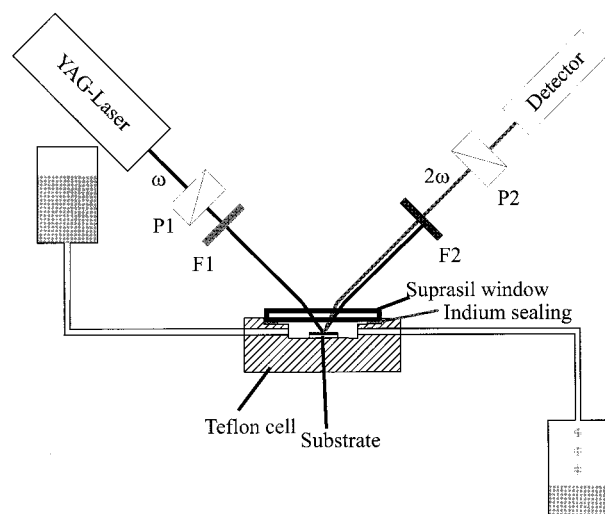


Figure 1. Scheme of the experimental setup of second harmonic generation at surfaces. P1 and P2 are polarizers, F1 and F2 are filters for blocking second harmonic and fundamental light, respectively. ω denotes the fundamental laser light at 1064 nm, 2ω the frequency-doubled light at 532 nm.

a boxcar averager, fed to an A/D converter, and stored in a computer for further evaluation. The energy of each laser pulse was measured with a pyroelectric detector, the output of which served to normalize the SHG signal of the sample. In all experiments both the incident fundamental and analyzed second harmonic beam were polarized parallel to the plane of incidence (pp polarization).

The adsorption experiments were performed in a home-built liquid cell consisting of a Teflon body and a Suprasil window sealed with an indium wire.⁴¹ The cell had a volume of about 500 μL and was connected to reservoirs. This allowed adsorption measurements under flow conditions; hence, any concentration gradients due to thiol depletion from solution which, particularly at low thiol concentrations, could distort the kinetic measurements are excluded. The substrates were placed parallel to the window at a distance of about 1–2 mm. The laser radiation was incident at an angle of 45° with respect to the surface of the cover glass.

The substrates were prepared by evaporating 100 nm thin layers of gold onto a Si(100) wafer with a 5 nm chromium adhesion layer. The wafer was cut into pieces of about 10 × 10 mm² which were used as samples. The cleanliness of the substrates was checked with XPS. Within the detection limit of XPS the gold surface was free of chromium. To minimize surface contamination the wafers were stored under argon until used. By means of this procedure only small amounts of carbon and oxygen could be detected on substrates which were immersed in pure ethanol. The gold film showed identical SHG properties for each sample and was used as substrate surface after multiple rinsing with ethanol and with the solvent used for the kinetics studies.

Prior to each experiment, all cell parts were carefully cleaned by first rinsing with absolute ethanol, then with 35% hydrogen peroxide, again with absolute ethanol, and finally with the pure solvent to be used in the adsorption experiments. After the substrate was mounted, the cell was sealed with the cover glass and then filled with pure solvent to align the optics. Adsorption was initiated by replacing the pure solvent with the solution containing the respective thiol. Due to the small volume of the cell the uncertainty of the zero point is reduced to less than 3 s. Since the thiol concentrations were in the micromolar region,

both liquids have identical optical properties, i.e., the same index of refraction which allows a direct comparison of the SHG signals from the gold substrate with and without thiol coverage. For concentration-dependent measurements, the thiol concentration was varied between 0.5 and 20.0 $\mu\text{mol/L}$. The signal-to-noise ratio of the SHG signal determines the time resolution of the experiment and imposes an upper limit in the thiol concentration which was about 10.0 $\mu\text{mol/L}$ for hexane. Solvent-dependent measurements were carried out with 2.0 μM solutions of docosanethiol ($\text{CH}_3(\text{CH}_2)_{21}\text{SH}$, C_{22}SH) in hexane (C_6H_{14}), dodecane ($\text{C}_{12}\text{H}_{26}$), hexadecane ($\text{C}_{16}\text{H}_{34}$), and ethanol (EtOH). The adsorption kinetics of thiols with different chain lengths was measured with docosanethiol, dodecanethiol ($\text{CH}_3(\text{CH}_2)_{11}\text{SH}$, C_{12}SH) and butanethiol ($\text{CH}_3(\text{CH}_2)_3\text{SH}$, C_4SH) in ethanol and hexane as solvents. Ethanol (Riedel-de Haën, $\geq 99.8\%$), hexane (Riedel-de Haën, $\geq 99\%$), dodecane (Fluka, $\geq 98\%$), and hexadecane (Fluka, $\geq 98\%$) were used without further purification. Docosanethiol ($\geq 99.7\%$) was prepared as described previously.⁴² Dodecanethiol (Fluka, $\geq 97\%$) and butanethiol (Aldrich, 99%) were used as received. In all experiments the flow rate was about 250 $\mu\text{L/s}$.⁴¹

3. Results

Analysis of SHG Data. The second harmonic signal from an adsorbate/substrate system is proportional to the absolute square of the total nonlinear susceptibility χ_{tot} which can be described by^{43–47}

$$\chi_{\text{tot}} = \chi_{\text{sub}} + \chi_{\text{int}}(\theta(t)) + \chi_{\text{ads}}(\theta(t)) \quad (1)$$

The subscripts denote the contributions originating from the substrate χ_{sub} , the adsorbate χ_{ads} , and their mutual interaction χ_{int} , and $\theta(t)$ is the time-dependent coverage. In our case, eq 1 simplifies to a superposition of the substrate and the interaction term. As verified experimentally,⁴⁸ χ_{ads} can be neglected in the case of alkanethiols due to the low hyperpolarizability of C–H bonds at a fundamental wavelength of 1064 nm.⁴⁹

To be able to extract quantitative information about the kinetics from the coverage-dependent SHG signal the explicit dependence of χ_{int} from θ must be known. A proportionality between χ_{int} and θ for two reasons cannot be assumed a priori but has to be verified experimentally. First, since the SHG signal traces the thiol adsorption through the changes in the nonlinear electronic properties of the gold surface caused by the Au–S bond formation, a nonlinear relationship between χ_{int} and θ is possible, particularly at high coverage where the average distance between the sulfur atoms becomes small enough for a mutual electronic interaction. However, experimentally only a linear relationship was found in comparative measurements using XPS.²⁷ Second, the susceptibilities are, in general, complex third-rank tensors; i.e., they are characterized by their magnitude and phase. If phase changes occurred due to changes of electronic resonances by thiol adsorption, a complicated coverage dependence of χ_{int} would result. Indeed, strong phase changes were observed for thiol adsorption on gold measured at a fundamental wavelength around 635 nm.^{50,51} In the case of $\lambda_{\omega} = 1064$ nm, however, there are no changes in the phase relation between χ_{sub} and χ_{int} as verified experimentally by interference experiments.²⁸ Furthermore, the phases of χ_{sub} and χ_{int} differ by 180° at this wavelength.²⁸ Since only the relative phases of χ_{sub} and χ_{int} are of interest we can define both as real. Thus, the dependence of the SH intensity from the thiol coverage is given by

$$I_{\text{SHG}} = A|\chi_{\text{sub}} - \chi_{\text{int}}^{(\theta=1)}\theta(t)|^2 I_{\omega}^2 \quad (2)$$

where A is a constant determined by the geometry of the experiment, the wavelength, and the dielectric constants.⁵² I_{ω} and I_{SHG} are the intensities of the incoming fundamental beam and of the second harmonic signal generated in reflection. The superscript of χ_{int} indicates the susceptibility of the interaction at the final coverage. The minus sign reflects the destructive interference of χ_{sub} and χ_{int} , i.e., $\chi_{\text{int}}(\theta=1) \geq 0$.

A convenient way to evaluate the experimental data is to normalize the SH signal to the value of the gold substrate prior to the thiol adsorption (χ_{sub}) which yields the simple expression

$$I_{\text{SHG}}^{\text{rel}} = [1 - R\theta(t)]^2 \quad (3)$$

with

$$R = \chi_{\text{int}}^{(\theta=1)}/\chi_{\text{sub}} \quad (4)$$

According to eq 3 all normalized SH spectra can be transformed to coverages according to

$$\theta(t) = \frac{1 - (I_{\text{SHG}}^{\text{rel}})^{1/2}}{R} \quad (5)$$

An example of an in situ thiol adsorption measurement is given in Figure 2a which shows the SHG raw data. As soon as the pure solvent is replaced by the thiol-containing solution, the SHG intensity starts to decrease and levels off at about 0.5. The corresponding time dependence of the coverage calculated from eq 5 is depicted in Figure 2b. The displayed data points represent the average of nine data points of Figure 2a.

We conclude this section with four remarks. First, since the SHG experiments monitor the initial, fast step of the formation of thiol films, we have not obtained in our experiments the final, maximum coverage but only 80%–90% of the final coverage.^{2,23,24} Consequently, the definition of $\theta = 1$ used throughout the paper is defined by the plateau reached after the first adsorption period. The second point is relevant for the mechanism of film formation discussed below. Since the literature proposes the existence of physisorbed and chemisorbed thiol molecules,^{38,53,54} the molecular interpretation of χ_{int} is of crucial importance. If physisorbed thiols contributed significantly to χ_{int} one would expect to see a change in signal upon exchange of the thiol containing solution by pure solvent at incomplete thiol coverage. If physisorbed species desorbed into the pure solvent the SHG signal should increase. Accordingly, a transition from a physisorbed state of the thiol into chemisorbed alkanethiolate species should lower the signal. Since neither is observed, one can conclude that SHG reflects the chemisorption of the thiol, i.e., the formation of the Au–S bond. Third, the total signal decrease depends on the value of χ_{sub} which could be affected by preadsorbed impurities. Therefore, the magnitude of $\chi_{\text{int}}(\theta=1)$ and the reproducibility of the signal decrease provides a means to judge the quality of the substrate. In our experiments the final signal levels were reproducible within $\pm 2.5\%$ which corresponds to a nominal variation in coverage of about $\pm 5\%$. Fourth, eq 2 is based on $\chi_{\text{int}}(\theta)$ being proportional to the thiol coverage. This cannot be assumed a priori. As for the phase relation between the tensor elements, this has to be verified experimentally. Calibration of the SHG signal with X-ray photoelectron spectroscopy has demonstrated such a linear relationship.²⁷

Phenomenology of Adsorption Kinetics. In the literature, four kinetic models have been proposed to describe the

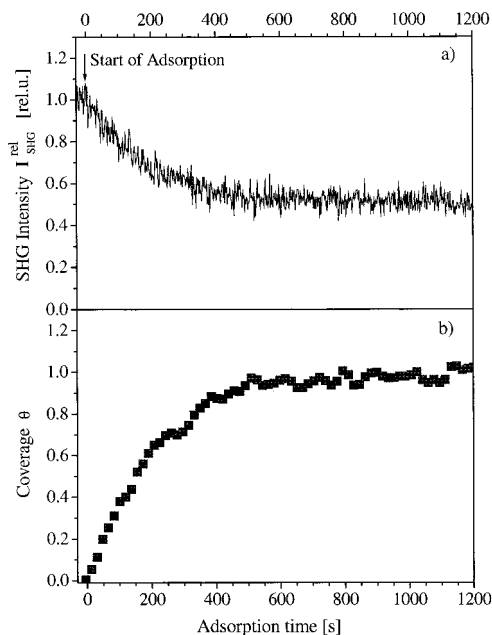


Figure 2. (a) Representative in situ SHG measurement of thiol adsorption. The example shows the adsorption of docosanethiol (C_{22} -SH) onto gold from 2.0 μM solution in ethanol. The fundamental wavelength is 1064 nm, the polarization is pp. (b) Time dependence of the coverage $\theta(t)$ (\blacklozenge) calculated from (a) using eq 5. One data point represent the average of nine data points from (a).

formation of thiol films. Since all models will be compared with our experimental data, we briefly summarize them. Simple Langmuir kinetics assuming an irreversible statistical adsorption process where⁵⁵

$$d\theta/dt \propto 1 - \theta \quad (6)$$

yields a time-dependent coverage

$$\theta(t) = 1 - e^{-ck_L t^a} \quad (7)$$

with $a = 1$. c and k_L are the concentration of the adsorbing species (in mol L^{-1}) and the rate constant of adsorption (in $\text{L mol}^{-1} \text{s}^{-1}$), respectively. Another description which in contrast to eq 6 takes the desorption into account³⁴ will be discussed in section 4. Accordingly, the time-dependent SHG signal is given by ($a = 1$)

$$(I_{\text{SHG}}^{\text{rel}})^{1/2} = R e^{-ck_L t^a} + (1 - R) \quad (8)$$

In addition to first-order Langmuir adsorption (LA) a diffusion-limited Langmuir model (LD) was suggested:³⁸

$$\theta(t) = 1 - e^{-ck_{LD} t^{0.5}} \quad (9)$$

which alters the time dependence of eq 8 to a $t^{0.5}$ dependence, i.e., $a = 0.5$. Furthermore, a second-order non-diffusion-limited model (SO) was proposed³⁸

$$\theta(t) = 1 - (1 + ck_{SO} t)^{-1} \quad (10)$$

which yields an SHG signal of

$$(I_{\text{SHG}}^{\text{rel}})^{1/2} = \frac{R}{1 + ck_{SO} t} + (1 - R) \quad (11)$$

The fourth model is based on purely diffusion-controlled

adsorption (DC).⁵⁶ The model used to describe the time dependence of the coverage is obtained by solution of the diffusion equation for semi infinite media with the boundary conditions of an initial concentration c above the substrate ($z > 0$, z as the coordinate along the substrate normal) and a vanishing concentration of free species at $z < 0$ at all times. This yields^{57,58}

$$\theta(t) = k_{DC} c t^{0.5} \quad (12)$$

where k_{DC} is given by

$$k_{DC} = \frac{2}{B_{ML}} \left(\frac{D}{\pi} \right)^{1/2} \quad (13)$$

D is the diffusion constant and B_{ML} is the number of particles per unit area at saturation coverage. Accordingly, the time dependence of the SHG signal is given by

$$(I_{\text{SHG}}^{\text{rel}})^{1/2} = -R k_{DC} c t^{0.5} + 1 \quad (14)$$

Since this model does not take into account saturation of the surface, it can only describe the initial stages of the adsorption where the rate of adsorption is approximately proportional to the flux of molecules onto the surface.

For the discussion below we mention an additional diffusion model, the boundary layer model (BL), which assumes a diffusion through a barrier of thickness d just above the surface. For $z > d$, the concentration c is identified with that of the thiol solution and does not depend on time; i.e., depletion of molecules in the bulk solution does not occur. For $z < 0$, the thiol concentration is zero. This yields a flux onto the substrate proportional to c .⁵⁷ With the assumption of Langmuir kinetics an equation formally equal to eqs 6 and 7 is obtained with ck_L being proportional to the diffusion constant D_{BL} of the barrier layer.

The agreement of the different models to describe the SHG data is demonstrated by Figure 3 showing the adsorption of docosanethiol from dodecane as solvent. The experimental data displayed in Figure 3a are replotted in Figure 3b,c to give a straight line according to eq 3 if the respective model holds. For the two Langmuir models the line must have a slope of +1 and has to originate at zero. For second-order kinetics its slope should be -1 and its intersection with the y-axis must be at $y = 1.0$. For the curves a rate constant k was chosen such that the data points come closest to the straight line. It is obvious that only the Langmuir model is consistent with our data.

Even though Figure 3 already demonstrates that among the models presented so far Langmuir kinetics describes the experiments best, the rate constant is a parameter which must be determined by a least-squares fit of the respective model to the experimental data. If the models do not exactly fit the data as is the case for three of the models, there is some uncertainty in defining the best rate constant. This uncertainty, however, is removed by concentration-dependent measurements. As demonstrated in Figure 4a, which shows the adsorption of docosanethiol from hexane at concentrations of 0.5, 2.0, and 10.0 $\mu\text{mol/L}$, an increase of the thiol concentration accelerates film formation. With these data the models can now be tested without fitting a rate constant. For an arbitrarily chosen value of the SHG intensity $I_{\text{SHG}}^{\text{rel}}$ (horizontal line in Figure 4a) the corresponding adsorption times $t_{\text{SHG},c}$ as a function of concentration can be determined (vertical arrows). Rewriting eqs 8, 11, and 14 such that (I, t) pairs of data are plotted versus concentration, the concentration dependence of the overall rate constant can

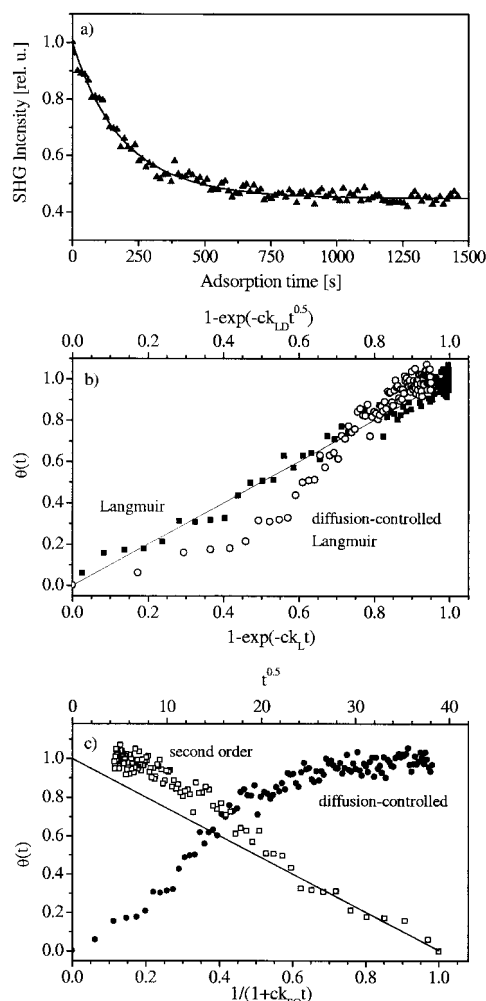


Figure 3. Adsorption of docosanethiol ($c = 2.0 \mu\text{mol/L}$) on gold from dodecane: (a) SHG signal (\blacktriangle) and a fit based on eq 8 ($R = 0.33$, $k_L = 2248 \text{ L mol}^{-1} \text{ s}^{-1}$). (b and c) Plots of the time-dependent coverage for different kinetic models. Abscissae are chosen such that for the respective model the experimental data should follow a straight line. For details see text.

be obtained. This is exemplified for the Langmuir model which writes as

$$\frac{-1}{t_{\text{SHG},c}} \ln \frac{R + (I_{\text{SHG}}^{\text{rel}})^{1/2} - 1}{R} = k_L c = \frac{-1}{t_{\text{SHG},c}} \ln[1 - \theta(t_{\text{SHG},c})] \quad (15)$$

The right-hand side of eq 15 follows from eq 5. The analogous forms for the other models are obtained straightforward and, thus, are not mentioned explicitly. The results for $I_{\text{SHG}}^{\text{rel}}$ 0.85, 0.75, and 0.57, which corresponds to coverages of $\theta = 0.26$, 0.44, and 0.80, are presented in Figure 4b–e. Note that for any particular concentration the data points have to coincide. Differences indicate that the model is inappropriate. Among the four models, again, only the Langmuir model is able to describe the data. As expected from eq 14, the data points are described by a straight line of slope k_L originating at zero and within the experimental uncertainty the data points for the different SHG intensities are at identical positions for a particular concentration. These criteria are met neither for the diffusion-controlled Langmuir (LD, Figure 4c) nor for the purely diffusion-controlled model (DC, Figure 4d). The DC model is expected to fail since it does not contain the self-termination of the adsorption process due to depletion of adsorption sites. Nevertheless, in the early

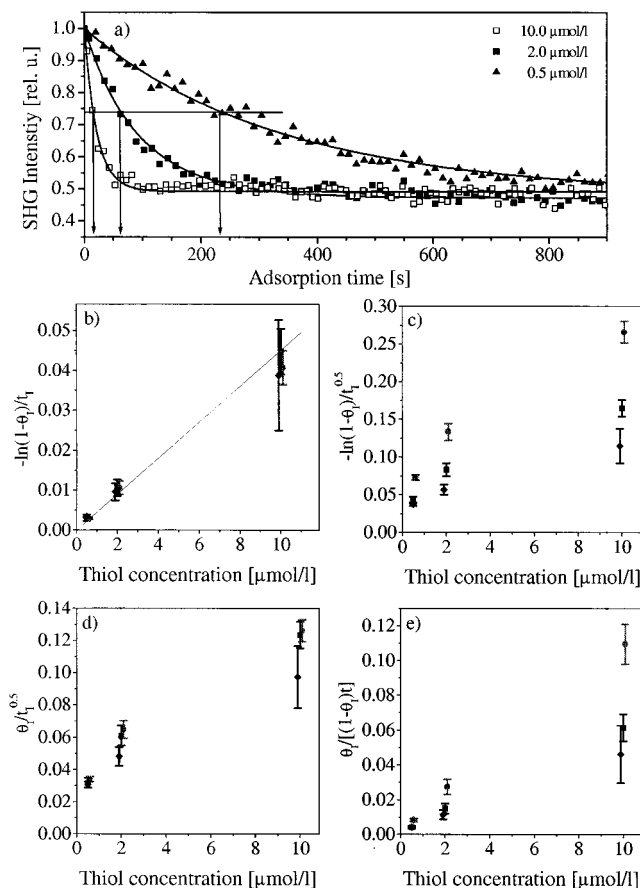


Figure 4. Concentration dependence of the rate constant of adsorption: (a) SHG signal of docosanethiol adsorbed onto gold from hexane solution. Solid lines are fits based on eq 8. The rate constants are compiled in Table 1. R is 0.306 ± 0.008 . (b–e) Test of different kinetic models. Data points represent pairs of a selected adsorption time and the corresponding SHG intensity which reflects the coverage. (\blacksquare) $I_{\text{SHG}}^{\text{rel}} = 0.57$ ($\theta = 0.80$), (\blacksquare) $I_{\text{SHG}}^{\text{rel}} = 0.75$ ($\theta = 0.44$), (\blacklozenge) $I_{\text{SHG}}^{\text{rel}} = 0.85$ ($\theta = 0.26$). For details see text.

stages of adsorption where this influence should be weak, the DC model could hold, and indeed the data of Figure 3c show a linear behavior for $\theta < 0.4$. However, the concentration-dependent data for $\theta = 0.26$ (diamonds) clearly deviate from a straight line and exclude diffusion-controlled adsorption even in the early stages of thiol adsorption. The failure of a diffusion controlled process is expected in the present case since a flow cell was used. However, as discussed in more detail in section 4, this is not a result specific for the present geometry but is likely to hold for other kinetic studies reported so far. For the second-order model (SO, Figure 4e) the data at a particular coverage are linearly dependent on the concentration c which suggests proportionality between c and the rate of adsorption k_{SO} . However, the slope is coverage dependent, invalidating the assumption of second-order kinetics.

With hexadecane as solvent an analogous concentration dependence is observed, except that adsorption proceeds significantly slower. For this reason the lower concentration limit was $2.0 \mu\text{mol/L}$ whereas the highest concentration studied was twice as high as in hexane. The rate constants obtained from a fit of eq 7 to the SHG data like those depicted in Figure 4a are compiled in Table 1. The errors are given by the standard deviation of the rate constants obtained from a number of up to four experiments per concentration. The linear dependence of the rate constant from the concentration has been shown previously for thiol adsorption from ethanol solution.⁴⁸

TABLE 1. Concentration Dependence of the Rate Constant k_L of the Adsorption of Docosanethiol onto Polycrystalline Gold from Hexane and Hexadecane^a

concentration	0.5 $\mu\text{mol/L}$	2.0 $\mu\text{mol/L}$	10.0 $\mu\text{mol/L}$	20.0 $\mu\text{mol/L}$
k_L ($\text{L mol}^{-1} \text{s}^{-1}$) in hexane	4985 ± 423	4588 ± 170	4596 ± 75	
k_L ($\text{L mol}^{-1} \text{s}^{-1}$) in hexadecane		1091 ± 87	1180 ± 105	1287 ± 114

^a Values are determined by least-squares fits of a Langmuir model (eq 7) to the SHG data.

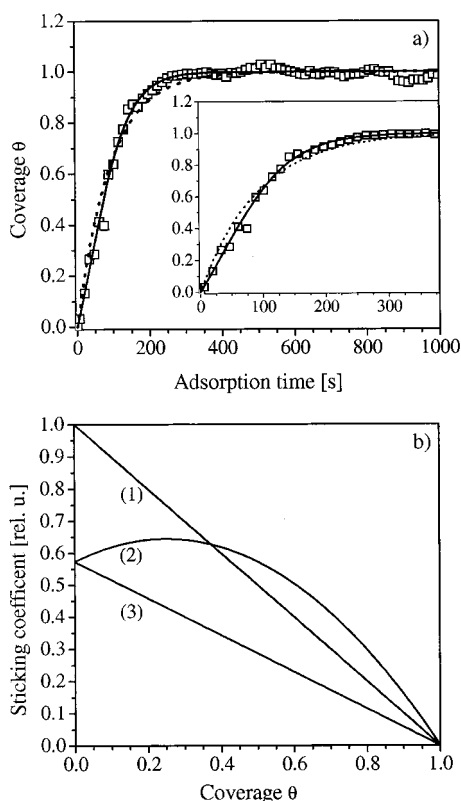


Figure 5. Adsorption of dodecanethiol from hexane: (a) time-dependent coverage determined from SHG measurements (\square) and fits based on Langmuir kinetics (dotted line, eq 7) and a precursor model (solid line, eq 17); (b) relative sticking coefficients for Langmuir kinetics (1), the precursor model (2), and its Langmuir part, only (3).

Despite the good general agreement between Langmuir kinetics and the experimental data, a closer inspection reveals that there are small but significant differences. These differences are found for all adsorption curves independent of concentration or solvent. As a representative example we will discuss the adsorption of dodecanethiol from hexane in more detail. Figure 5 displays the experimental data together with fits based on the Langmuir model (dotted line). The solid line represents a model to be presented below. In the initial stages of adsorption ($t < 100$ s) the Langmuir model predicts a slightly faster increase in coverage than found experimentally. Conversely, at coverages $\theta > 0.80$ the fit gives lower coverages than the experimental data points. Analogously, in Figures 7a and 8a which display the SHG intensity instead of the coverage the fits decrease too fast at first and then too slowly. This systematic deviation from experiment can be removed by refining the model. Motivated by STM/AFM experiments in which an island type growth of the thiol layers was observed^{53,54,59} we replace the simple Langmuir kinetics by a modified Kisliuk model (KM).^{60,61} As depicted in Figure 6 this model assumes different pathways for a molecule to chemisorb. One route, described by a sticking

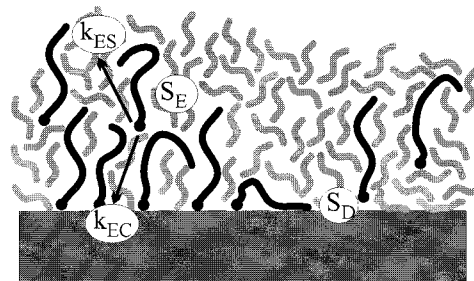


Figure 6. Illustration of our proposed model of the rate-limiting step of alkanethiol adsorption from solution, the modified Kisliuk model. Two different pathways for a molecule to chemisorb exist. The first route refers to molecules approaching areas free of thiol molecules. The displacement of preadsorbed solvent molecules, described by a sticking coefficient $S_D(\theta)$, is rate limiting. Another route describes thiol molecules impinging onto thiolate islands. Since the interaction of a thiol molecule with a thiolate island is likely to be different from its interaction with the surface covered only by solvent molecules, a precursor species with a sticking probability $S_E(\theta)$ is assumed. From this intermediate state the thiol molecule can be either incorporated into the island and transform to a thiolate at a rate k_{EC} or desorb at a rate k_{ES} .

coefficient $S_D(\theta)$, is the adsorption of thiol molecules onto areas free of molecules of alkanethiolate already adsorbed. Another route describes thiol molecules impinging onto thiolate islands. Since the interaction of a thiol molecule with a thiolate island is likely to be different from its interaction with the surface only covered by solvent molecules, a precursor species with a sticking probability $S_E(\theta)$ different from $S_D(\theta)$ is assumed. From this intermediate state the thiol molecule can either be incorporated into the island and transform to a thiolate at a rate k_{EC} , or desorb at a rate k_{ES} . Note that k_{ES} describes the desorption of an intact thiol molecule and is not the rate constant of desorption of a thiolate adsorbed on the substrate. Such a model which has been discussed in detail for UHV studies yields a coverage-dependent sticking coefficient and the rate of adsorption is described by⁶⁰

$$\frac{d\theta}{dt} = c \left[S_D^{\theta=0} (1 - \theta) + S_E^{\theta=0} \theta \frac{k_{EC}(1 - \theta)}{k_{ES} + k_{EC}(1 - \theta)} \right] \quad (16)$$

If one assumes that desorption from the precursor state is much more likely than transformation to a chemisorbed thiolate, k_{ES} is much larger than k_{EC} and eq 16 can be simplified to

$$d\theta/dt = ck_L(1 - \theta)(1 + k_E\theta) \quad (17)$$

with k_L and k_E incorporating rate constants and the sticking probabilities. $k_E\theta$ describes the deviation from Langmuir kinetics due to changes of the overall sticking coefficient by adsorbed thiolate. Analogous to eq 6, eqs 16 and 17 assume that the rate of desorption of thiolates is negligible. Integration of eq 17 yields

$$\theta = \frac{e^{(1+k_E)ck_Lt} - 1}{e^{(1+k_E)ck_Lt} + k_E} \quad (18)$$

As indicated by the solid line in Figure 5, eq 17 represents a significantly better description of the SHG data. For the example shown here, k_L and k_E are $3150 \text{ L mol}^{-1} \text{s}^{-1}$ and 2.0, respectively. Since k_E accounts for the adsorption from the island precursor state, the result shows that thiolate molecules already present on the surface significantly promote the adsorption of additional thiol molecules. In Figure 5b a comparison between

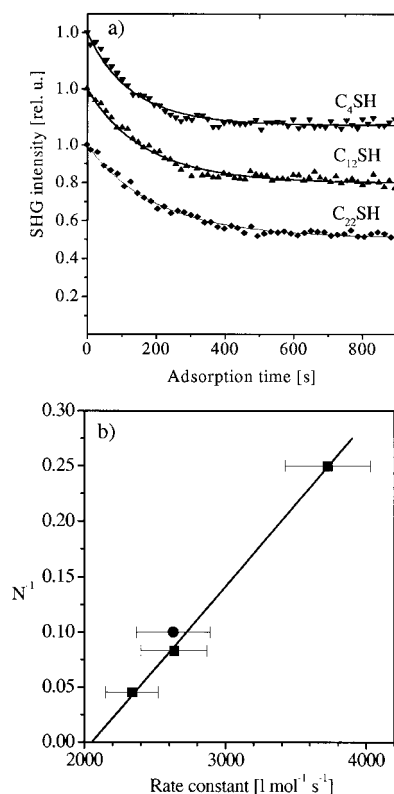


Figure 7. Chain length dependence of the thiol adsorption on gold from ethanol: (a) Solid lines are fits to the SHG data (symbols) based on eq 8 ($R = 0.290 \pm 0.003$). The rate constants are compiled in Table 2. (b) Plot of the rate constants vs inverse of the chain length. The data point represented by the solid circle (●) is taken from ref 73 and represents decanethiol. For details see text.

different sticking probabilities is shown. Line 1 results from the Langmuir fit, line 3 and line 2 represent the Langmuir contribution of eq 17 ($k_E = 0$) and the total sticking probability ($k_E = 2.0$), respectively. As addressed in more detail in section 4, we have no information about the flux of molecules onto the surface and thus only relative values of the sticking probability can be given. It is obvious that the two models yield sticking probabilities which are significantly different, particularly for $\theta < 0.4$. The value of $k_E = 2.0$ was found to be typical for all experimental conditions but can be varied by about 30% (with readjustment of k_L at the same time) without affecting the quality of the fits significantly. We have not found any systematic changes of k_E upon variation of the experimental parameters investigated, i.e., chain length, solvent, or concentration. Therefore, despite its limitations, the Langmuir model is suitable to evaluate the functional dependence of the rate of thiol adsorption from the experiments since the ratio between the rate constants of the pure Langmuir and the precursor model is constant.

Chain Length and Solvent Dependence. In Figures 3 and 4 it was shown that diffusion-controlled adsorption as described by the DC model cannot be the correct mechanism. However, diffusion through a boundary layer as described by the BL model mentioned above would be consistent with the experiments presented so far. A diffusion through such a boundary layer is expected to depend on both the size of the thiol molecule and the nature of the solvent. The results for the variation of the chain length of the thiols are shown in Figures 7 and 8. In Figure 7a (8a) the SHG intensity for the adsorption of $C_m\text{SH}$ ($m = 4, 12, 22$) from ethanol (hexane) is plotted versus time. Neglecting the small deviations discussed above, Langmuir kinetics (solid

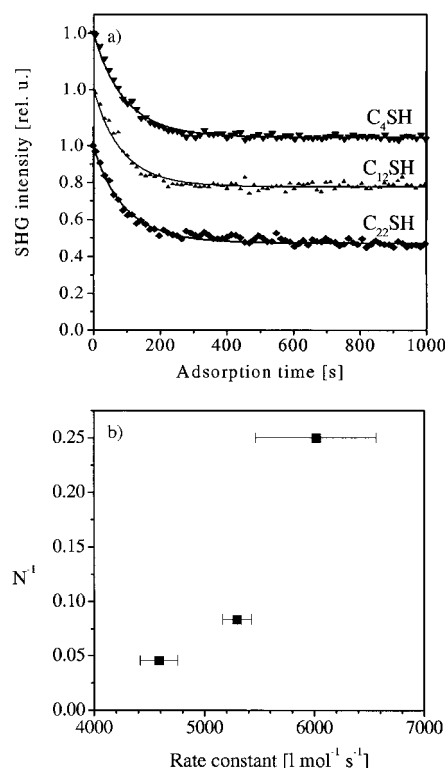


Figure 8. Chain length dependence of the thiol adsorption on gold from hexane: (a) Solid lines are fits to the SHG data (symbols) based on eq 8 ($R = 0.320 \pm 0.013$). The rate constants are compiled in Table 2. (b) Plot of the rate constants vs inverse of the chain length N . For details see text.

curves) describes the data quite well. From the two figures and Table 2 listing the fitting parameters it is evident that for both the polar and the nonpolar solvent the rate constant decreases with increasing chain length. This chain length dependence of the rate constant describing the first step of film formation is in agreement with the AFM studies of Tamada et al.⁵³ and opposite to the behavior reported for the time needed to form a complete monolayer. In contact angle measurements the limiting value for a completed monolayer was reached faster with hexadecanethiol ($C_{16}\text{SH}$) compared to decanethiol ($C_{10}\text{SH}$).² For the discussion of different models of thiol adsorption with respect to the chain length dependence (see section 4) we plot the dependence of the rate constant from the chain length as a function of the inverse of the chain length (Figures 7b and 8b). This representation is motivated by molecular dynamics simulations⁷² and is based on the reptation model⁶² which predicts the mobility of the molecules to scale with N^{-1} . Whereas proportionality is found for ethanol, no simple relationship is obtained for hexane.

The influence of the *solvent* was studied using a 2.0 μM solution of docosanethiol in *n*-alkanes of different chain lengths. Alkanes were chosen since they allow to systematically vary the size of the molecule and the viscosity of the solvent without altering other solvent properties, e.g. polarity. From the adsorption curves analogous to Figures 7a and 8a the rate constants were derived and are compiled in Table 3. A solvent dependence of the rate constant is clearly observed as can be seen from Figure 9 where the results in different representations are displayed. If the diffusion barrier for the thiol is described by a standard Stokes–Einstein relation, a scaling of the rate constant with η^{-1} is expected.⁶³ Figure 9a shows that this is not the case. Empirically, the data are found to be described best by a $\eta^{-0.63 \pm 0.3}$ dependence. For comparison the rate constant

TABLE 2. Rate Constant k_L of the Thiol Adsorption onto Polycrystalline Gold from Hexane and Ethanol as a Function of Chain Length^a

adsorbate	butanethiol (C ₄ SH)	dodecanethiol (C ₁₂ SH)	docosanethiol (C ₂₂ SH)
k_L (L mol ⁻¹ s ⁻¹) in ethanol	3726 ± 304	2636 ± 234	2337 ± 187
k_L (L mol ⁻¹ s ⁻¹) in hexane	6017 ± 547	5298 ± 131	4588 ± 170

^a Values are determined by least square fits of a Langmuir model (eq7) to the SHG data.

TABLE 3. Solvent Dependence of the Rate Constant k_L of the Adsorption of Docosanethiol onto Polycrystalline Gold^a

solvent	hexane	dodecane	hexadecane	ethanol
rate constant k_L (L mol ⁻¹ s ⁻¹)	4588 ± 170	2248 ± 28	1091 ± 87	2337 ± 187
viscosity η (mPa·s) at 20 °C	0.326	1.30	3.34	1.20

^a Values are determined by least square fits of a Langmuir model (eq7) to the SHG data.

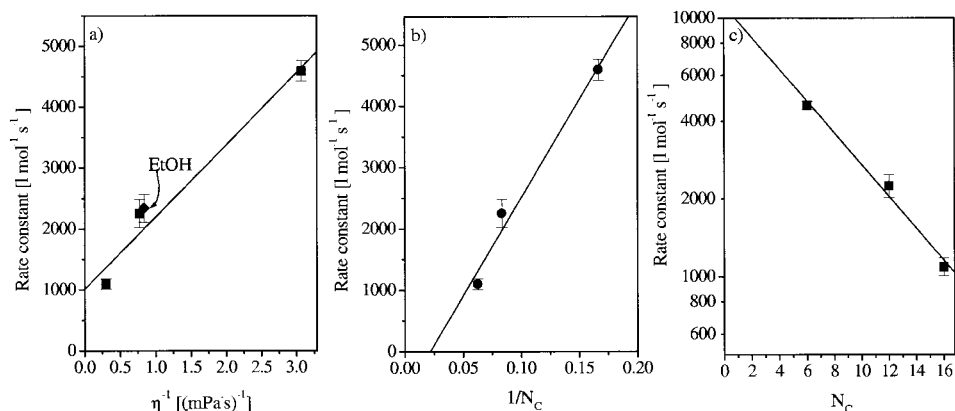


Figure 9. Adsorption of docosanethiol on gold from solvents of hexane, dodecane, and hexadecane. Plot of the rate constant vs the viscosity (a), the inverse of the solvent chain length (b), and logarithmic plot of the rate constant vs the chain length of the solvent (c). For details see text.

for adsorption of docosanethiol from ethanol has been included in Figure 9a. Interestingly, the rate constant found for thiol adsorption from ethanol is equal to that from dodecane, both solvents having the same viscosity (see Table 3). However, we consider this agreement fortuitous, since, as will be discussed below, normal diffusion is not considered rate-limiting. A satisfactory linearity is achieved by plotting k_L vs the inverse of the number of carbon atoms of the solvent N_C (Figure 9b). As above, this representation is based on the reptation model. A third relation being discussed below in more detail assumes that solvent molecules adsorbed on the surface play a crucial role in the process of thiol adsorption. In the plot of Figure 9c a thermally activated process

$$k_L = k_0 e^{-N_C E/kT} \quad (19)$$

is assumed to influence the residence time of the solvent molecule adsorbed at a particular surface site. The underlying microscopic picture is that the residence time of a molecule adsorbed on a surface scales with its size. In other words, the activation energy for lateral diffusion of an adsorbed molecule is dependent on the number of methylene/methyl groups interacting with the substrate.

4. Discussion

Langmuir adsorption kinetics of alkanethiols onto gold substrates was found by various techniques such as surface plasmon resonance,³⁷ quartz crystal microbalance,^{33,34} surface acoustic waves,²⁶ and a micromechanical stress sensor.⁶⁴ In the latter two cases adsorption from the gas phase was studied. Even though the reports for adsorption from solution agree with respect to the kinetic model, there are large differences in the quantitative interpretation. A rate constant drastically different from our data was reported by Pan et al.³³ who found a rate

constant about 3 orders of magnitude larger. Furthermore, there were substantial deviations from the Langmuir behavior. A somewhat better agreement with our results exists with the data reported by DeBono et al.³⁷ who used ethanol as a solvent. However, their values are still lower by a factor of 2.5–5. Among the in situ experiments, our rate constants agree best with those of Karpovich and Blanchard.^{34,65} For octadecanethiol adsorbed from hexane they report values for the rate constant of adsorption in the range of 2100 to 2400 L mol⁻¹ s⁻¹ which is roughly a factor of 2 smaller as compared to our value of about 5000 L mol⁻¹ s⁻¹ (Table 2). This difference can be considered minor and can be easily explained (see below). There is, however, a substantial disagreement with our results concerning the presence of a desorption channel. Karpovich and Blanchard assume the desorption of thiols to be a first-order reaction which results in the following expression for the stationary adsorption–desorption equilibrium³⁴

$$k_L c(1 - \theta) = k_d \theta \quad (20)$$

where k_d is the rate constant of desorption. With their values of 2440 L mol⁻¹ s⁻¹ for k_L and 0.19 s⁻¹ for k_d , an equilibrium coverage of $\theta = 0.13$ ($\theta = 0.00152$) results at a thiol concentration of 10 μ mol/L (0.5 μ mol/L). This is grossly incorrect since our data clearly show that the final level of the SHG intensity is independent of concentration (see for example Figure 4). Furthermore, assuming such a rate constant of desorption, a thiol film of $\theta = 1$ should deteriorate to $\theta = 0.01$ within less than 30 s. Since this is not observed experimentally, the only speculative explanation would be that at high coverage there is a dramatic increase of the stability of the film; i.e., k_d would have to drop drastically. Even though experiments using ³⁵S-labeled thiols show a substantial loss of thiols in pure solvents such as hexane, the time scale is on the order of at

least 1 day.⁵⁶ Furthermore, as mentioned above, in some of our adsorption experiments the thiol solution was replaced by pure solvent at incomplete coverage. This did not cause any changes in the SHG signal. Thus, thiols do not desorb easily, even at submonolayer coverage and, in contrast to the QCM experiments reported,³⁴ the desorption of thiolates is negligible within the accuracy of our technique and the time scales considered here.

In addition to the *in situ* studies of film formation discussed above, there are two *ex situ* studies using IR spectroscopy.^{24,39} Even though no exact values for the rate constants are given, the time reported by Truong and Rowntree for the completion of the first rapid step of film formation (~ 5 min at $5 \mu\text{mol/L}$ for butanethiol in methanol) agrees well with our experiments (see Figure 7).²⁴ Bensebaa et al. give values which seem to be somewhat higher but on the same order of magnitude (45 s at $5 \mu\text{mol/L}$ for docosanethiol in ethanol).³⁹ Since in IR spectroscopy information about the coverage is mixed with the orientation of the molecules, we postpone a detailed discussion of results from vibrational spectroscopy to a forthcoming publication where film formation is studied by IR-vis sum frequency generation, a nonlinear vibrational spectroscopy which allows a direct correlation of the coverage and the vibrational spectrum.⁶⁶

Despite most of the *in situ* studies reported simple Langmuir kinetics, based upon experimental data, other mechanisms of film formation were proposed. Schlenoff et al. concluded from the agreement between their *ex situ* kinetic data and a calculation using a typical bulk diffusion coefficient that adsorption is controlled by diffusion.⁵⁶ Besides for the reason outlined already above pure, diffusion control can in principle not describe thiol adsorption up to the final coverage, the concentration-dependent experiments presented here show that even at low coverage diffusion does not control the rate (Figure 4). Two other models were suggested describing the results of SPR experiments,³⁸ one of which is a diffusion-controlled Langmuir adsorption (eq 9), and the other one a second-order reaction (eq 10). As shown in Figures 3 and 4, these models cannot account for our data. The origin of the discrepancies between these SPR experiments and our SHG studies is not clear. The most obvious difference is that different techniques were used in the adsorption experiments. SHG is only representative of the thiolate coverage since it probes changes in the electronic properties of the gold surface caused by thiolate formation and thus is insensitive to processes above the immediate Au-S interface, i.e., to conformational changes of the molecules or changes in the index of refraction. In contrast, due to the relatively large decay length of the electric field of the surface plasmon above the surface, SPR probes the optical properties of the whole thiol layer. However, this can hardly be the only reason for the discrepancies since there is another SPR study which is quite comparable with respect to the thiols and solvents used and which reports simple Langmuir kinetics.³⁷ Furthermore, the extremely weak dependence of the rate constants on the thiol concentration is not clear³⁸ and is not only contrary to our present results but also to other *in situ*^{27,37} and *ex situ* studies.^{2,30}

Even though the experiments reported in the literature and those presented here can be described well by Langmuir kinetics for a broad range of experimental conditions, i.e., for different solvents and chain lengths, it appears surprising that such a simple model explains a complicated system as *n*-alkanethiols adsorbing on gold. One basic assumption of the simple Langmuir model—that is, the adsorption sites are not affected

by the local coverage of the adjacent sites—is not reasonable considering the size of the molecule (e.g. docosanethiol fully extended $\sim 30 \text{ \AA}$) relative to the average distance of the adsorption sites (5 \AA). Furthermore, the high degree of structural order in completed alkanethiolate films shows that the interactions between adjacent molecules are essential for the structural properties of thiol layers. As mentioned in the Introduction, SAM formation is not a single-step process.^{2,23,37} There is general agreement that a fast initial phase described by Langmuir kinetics is followed by a second or even third step proceeding much slower. However, already during the initial step the coverage increases already to a density of $\theta = 0.8\text{--}0.9$,^{2,23,24,37} where the assumption of independent adsorption sites seems not to be justified. Indeed, as our analysis of the SHG data suggests (Figure 5) there is a deviation from Langmuir kinetics for $\theta < 0.8$ which can be accounted for by a coverage dependence of the rate constant (eqs 16–18). Considering the small difference between the pure and the modified Langmuir model, it is not surprising that, due to the limited accuracy of the methods used to study the kinetics of thiol film formation, pure Langmuir kinetics provides a sufficiently precise phenomenological description. Taking into account that different adsorption channels might be present, one would expect that the ratio of the respective rate constants is dependent on the details of the system, i.e., on the interactions between the thiol molecules themselves and with the solvent. In the experiments presented here, we could not identify any systematic change in the ratio of the rate constants associated with the two adsorption channels. k_E is always about 2.0, independent of the chain length, the concentration, or the solvent. This does not mean that there are no differences but rather indicates that the signal-to-noise ratio has to be improved to allow a more detailed statement. For a different system there are more pronounced indications that the details of the kinetics are system dependent. For *p*-nitroanilindodecanethiol, an alkanethiol with a highly dipolar endgroup, we see differences between the adsorption from ethanol and hexane.⁶⁷

The assumption of a model which takes into account two adsorption channels is substantiated by recent studies of thiol adsorption from solution using AFM^{53,54} and STM.⁵⁹ The mechanism of film formation from solution seems to be qualitatively identical to adsorption from the gas phase.⁶⁸ All three studies find the formation of islands after an initial period of adsorption and their growth until coalescence. The height of the islands suggests that they consist of upright standing thiols. In the initial stages of adsorption, i.e., at low coverage, a striped phase forms in which the molecules are lying flat on the surface.^{54,59,68–70} Subsequently a phase transition occurs and islands of upright standing thiols are formed which continue to grow with thiol exposure. Island formation cannot be explained by a statistical adsorption model, but is in agreement with the model including cooperative effects for a precursor (Figure 6).

Tamada et al.⁵³ suggested that a physisorbed intermediate state, during which the domains of upright standing thiols form, precedes the covalent attachment of the thiol to the substrate. This mechanism was proposed to fit their observation of island formation with the literature^{26–28,33,34,37,64} which reported Langmuir kinetics, i.e., random adsorption. In that model the physisorbed state has to exist for a relatively long time in order for the molecules to be able to move over significant distances to form islands. This qualitative scheme was more detailed by Xu et al.⁵⁴ who quantified the different adsorption states. After an initial delay the physisorbed state prevails up to a coverage of 80%–90% and only subsequently transforms to the chemi-

sorbed phase. Formation of the physisorbed lying-down phase is described by Langmuir kinetics whereas formation of the upright phase could be fitted either by a Langmuir isotherm or by a second-order model. In their model it remained open when exactly the transition from a physisorbed to a chemisorbed phase occurs.⁵⁴

For a comparison of STM/AFM and SHG experiments we recall that SHG detects the formation of the Au–S bond, i.e., the change of the second harmonic signal is due to thiolate formation and not to physisorption of the thiol. The SHG experiments show that chemisorption of thiols occurs right from the beginning (Figure 2). Even though we cannot exclude a physisorbed state prior to the transition into the chemisorbed state, its lifetime must be short with respect to the time resolution of our experiment which is a few seconds. Thus, our experiments are at variance with those of Xu et al. who report an induction period.⁵⁴ Unfortunately, the time scales of both experiments are very different and thus a direct comparison is impossible. In agreement with our SHG experiments, Tamada et al.⁵³ and Yamada and Uosaki⁵⁹ reported that the surface was completely covered with the islands after 3 min for a 10 μ molar solution of C₁₂SH in EtOH⁵³ and 10 min at 2 μ mol/L for C₁₀SH in heptane, respectively.⁵⁹ In contrast, Xu et al.⁵⁴ report the onset of island formation after 7.5 min at a concentration of 200 μ mol/L for 2-butanol which is about a factor of 20 slower than found in the other experiments. The origin of this difference is not clear but could be due to different conditions (e.g. cleanness) of the gold surface. Nevertheless, despite the quantitative differences island formation is a common observation in the microprobe experiments. However, a long-living physisorbed state is not required to explain these results. As demonstrated in our SHG experiments a chemisorbed state forms instantaneously and island formation can be explained by precursor states with different sticking probabilities. The immediate formation of a chemisorbed state is also suggested by experiments using atomic absorption spectroscopy.^{15,71} Dissolution of gold which indicates a strong thiol gold interaction was found in the initial stages of thiol adsorption. We close this point of the discussion by noting that in deriving eq 18, $k_{ES} \gg k_{EC}$ was assumed since it allows analytical integration of eq 16. The very good agreement between the data and eq 18 does not ultimately prove that this condition is fulfilled. How well this assumption holds cannot be decided at present since k_E can be varied by about 30%. An improved signal-to-noise ratio is required to clarify this point.

In addition to the sticking coefficient, the flux of thiols onto the surface determines the rate of the film formation. As shown by the SHG experiments, a purely diffusion-limited process (DC) can be ruled out. However, as pointed out above, a barrier layer described within the framework of classical diffusion is, in principle, consistent with the experimental results, i.e., the concentration dependence of the rate constant. For a rough estimation whether such a barrier between the bulk of the solution and the substrate gives a meaningful concept we describe the diffusion-limited flux F through a plane sheet by⁵⁷

$$F = D_{BL}(c_b - c_s)/d \quad (21)$$

with d as the thickness of the diffusion layer and D_{BL} as the diffusion constant which is assumed to be independent of the thiol concentration, a reasonable assumption for the concentrations used in our experiments. c_b is the thiol concentration above the layer. c_s which denotes the concentration right at the substrate has to vanish since the thiol molecules transform irreversibly to thiolates. In our experiments the formation of a

monolayer ($\sim 5 \times 10^{14}$ molecules/cm²) takes about 10^{-3} s which corresponds to a flux of $5 \times 10^{11-12}$ molecules/(cm²s). Taking a typical value of 10^{-5} cm²/s for D_{BL} and a bulk concentration of 2 μ mol/L, a value of d in the range of 10^{-2} – 10^{-3} cm results. This value of d is unreasonably large considering the fact that adsorption takes place under flow conditions. In other words, if the adsorption process were controlled by such a diffusion barrier, the flux of molecules and, hence, the rate of thiol adsorption should be much higher than observed.

Of course, this calculation depends critically on the value of the diffusion constant. Near interfaces the diffusion constant can be significantly different from the bulk value as shown by a molecular dynamics (MD) simulation of Xia and Landman.⁷² However, the deviation of the diffusion constant from its bulk value becomes appreciable for d below 10^{-6} cm. Such a small value requires unreasonable values of D_{BL} in eq 21, at least 3 orders of magnitude smaller compared to the bulk value to fit with the rate constant determined by SHG. Therefore, a different process seems to be required as the rate-limiting step. Before suggesting an explanation of the rate-limiting step we close the discussion on diffusion by adding a few remarks. First, eq 21 describes a net flux of molecules onto the surface and does not make any assumptions about collision rates of the thiol molecules with the substrate or about sticking coefficients. It is merely the solution of the classical diffusion equation with boundary conditions of zero thiol concentration at the substrate/barrier interface and the bulk concentration of the thiol at the barrier/bulk interface. The second point relates to the first one and addresses the magnitude of the sticking coefficient. In Figure 5b we gave relative values for the different models. Unfortunately, no absolute values can be given since the flux of thiol molecules onto the surface is not known. The differential equations of diffusion correlate the flux with concentration gradients and the diffusion coefficient. At interfaces both quantities are difficult to control and/or are not known. As the above estimations may have demonstrated, a variation over several orders of magnitude is easily possible. Microscopic models based on molecular dynamics simulation may provide further insight. Third, we like to note that our experiments do not prove that diffusion cannot be involved in the rate-limiting step under any experimental circumstances. Nevertheless, it would be experimentally difficult to realize a situation where the conditions are such that diffusion can be clearly separated from other effects. Convection and turbulence must be carefully excluded and considering the way thiol adsorption takes place, i.e., by immersion of the substrate in the thiol solution or by pouring the thiol into the solvent, this would be hard to control. For this reason we took the opposite approach and purposely eliminated any possible contributions from diffusion by use of a flow cell. However, we also performed experiments in cells of different geometries and without flow.⁷⁵ Compared to the flow cell experiments, the same rate law was found even at low concentrations where the effect of diffusion should be most pronounced. Since in all the experiments reported in the literature no particular attention was paid to control thiol adsorption with regard to diffusion, we claim that under usual adsorption conditions diffusion is not important.

Considering bulk diffusion irrelevant for the kinetics we propose the penetration of the alkanethiol molecule through the interphase to the gold surface as rate limiting that is the displacement of the solvent molecules and/or the incorporation into an island of upright standing thiols. According to the precursor model discussed above (eqs 16–18) two different pathways exist for a thiol molecule to chemisorb. For thiol

molecules impinging onto thiolate islands the penetration through this thiolate layer onto the gold substrate would be rate limiting. For molecules arriving at sites free of thiolates the displacement of the solvent molecule from the surface is considered rate limiting. In both cases creation of adsorption sites is the decisive process. This model is consistent with the observation that docosanethiol adsorbs significantly faster than didecyl disulfide ($\sim 60\%$, normalized to the number of thiol units).⁷³ Having about the same molecular size the former requires only one adsorption site whereas the latter needs two and thus has a lower probability of being chemisorbed. Further support of the model that the rate-limiting step is associated with the chemisorption step is the observation that upon aging of the substrate, i.e., long exposure to the ambient atmosphere which results in the formation of a contamination layer of hydrocarbons, the rate constant of adsorption is reduced.⁷⁴ Therefore, in addition to the displacement of solvent molecules, removal of such hydrocarbon contaminations which, with respect to the mechanism, is identical to the solvent case may also be involved in the rate-limiting steps.

Finally, the question remains how the chain length of the thiol molecules and the solvent dependence fit into the proposed model. Generally, the mobility of an alkanethiol will be influenced by its chain length. Considering that the whole system is highly dynamic, the chance for a thiol molecule impinging on a surface site where a solvent molecule has moved and opened up an adsorption site, or where thiolates separate and allow the thiol molecule to be incorporated into the island, should scale with the mobility which decreases with increasing chain length. However, a quantitative understanding requires a detailed modeling of the interfacial processes.

Considering the complexity of phenomena in the vicinity of interfaces, e.g. deviations of a liquid from its bulk structure and mobilities of molecules different from the bulk, it is not surprising that the agreement between the simple model and the data presented in Figures 7b and 8b is strongly dependent on the solvent, i.e., exhibit a pronounced difference between EtOH and hexane. It does not prove or disprove the appropriateness of the reptation model but rather demonstrates that the solvent plays a decisive role in the mechanism of film formation. We stress again that the motivation for the reptation model comes from MD simulations of alkanes, i.e., molecules which have a structure very similar to thiols. Their interaction with a gold surface yields a reptation-like behavior.⁷² To what extent this is a meaningful concept for the formation of thiol monolayers cannot be decided at present and needs further, in particular theoretical, investigations.

The explanation of the solvent dependence is intimately connected with the mechanisms just discussed. Consistent with the above arguments that bulk diffusion does not play a role is the observation that the viscosity is not a good parameter to describe the solvent effect (Figure 9a). Since an equally good agreement between the data and the two other models (reptation-like, Figure 9b, and thermally activated, Figure 9c) is observed, a differentiation is impossible. It might be that even both of the underlying mechanisms are involved due to the fact that the substrate is inhomogeneously covered with thiolate during film formation. On thiolate-free areas eq 20 might be valid since the solvent is adsorbed on the substrate and has to move to free an adsorption site. In contrast, at the thiolate islands solvent molecules can be incorporated and thus their mobility, which is expected to scale according to the reptation model, should affect the adsorption rate (k_{EC}) of thiols.

5. Conclusion

In situ SHG studies of the adsorption of *n*-alkanethiols from solution onto gold revealed that among various kinetic models presented in the literature only simple Langmuir adsorption kinetics satisfactorily describes all the data, independent of chain length, solvent, and thiol concentration. Nevertheless, as revealed by a more detailed analysis of the SHG data, a refined precursor model which takes different types of adsorption sites into account is required. This model also explains island formation identified by scanning probe techniques. Our data do not give any evidence that a long-living intermediate physisorbed species does exist and is required for islands to form. Differences in the rate constants for thiols and disulfides, the failure of any diffusion based model, and studies of the solvent dependence lead to the conclusion that the processes at the immediate interface are rate-limiting. Nevertheless, a number of points such as the quantitative understanding and mechanistic details of the solvent effects and the chain length dependence are still open and will require additional experimental investigations in combination with MD simulations.

Acknowledgment. We thank F. Eisert and H. J. Kreuzer for valuable discussions, and A. Lampert and R. Kohring for the program used for data acquisition and evaluation. We gratefully acknowledge W. Schrepp and H. Kullmann, BASF AG, and H. Schwenk, Wacker Siltronic, for providing the substrates. This work was funded by the Deutsche Forschungsgemeinschaft and the Fonds der Chemischen Industrie.

Glossary

AFM	atomic force microscopy
BL	boundary layer model
C ₆ H ₁₄	hexane
C ₁₂ H ₂₆	dodecane
C ₁₆ H ₃₄	hexadecane
C ₂ SH	ethanethiol (CH ₃ (CH ₂) ₁ SH)
C ₄ SH	butanethiol (CH ₃ (CH ₂) ₃ SH)
C ₁₂ SH	dodecanethiol (CH ₃ (CH ₂) ₁₁ SH)
C ₂₂ SH	docosanethiol (CH ₃ (CH ₂) ₂₁ SH)
DC	diffusion-controlled adsorption
EtOH	ethanol
EQCM	electrochemical quartz crystal microbalance
FTIRRAS	Fourier transform infrared reflection absorption spectroscopy
KM	Kisliuk model
LA	Langmuir adsorption
LD	diffusion-limited Langmuir model
ML	monolayer
NEXAFS	near-edge X-ray absorption fine structure
QCM	quartz crystal microbalance
SAM	self-assembled monolayer
SFG	sum frequency generation
SHG	second harmonic generation
SO	second-order nondiffusion-limited model
SPR	surface plasmon resonance
STM	scanning tunneling microscopy
XPS	X-ray photoelectron spectroscopy

References and Notes

- (1) Nuzzo, R. G.; Allara, D. L. *J. Am. Chem. Soc.* **1983**, *105*, 4481–4483.

- (2) Bain, C. D.; Troughton, E. B.; Tao, Y.; Evall, J.; Whitesides, G. M.; Nuzzo, R. G. *J. Am. Chem. Soc.* **1989**, *111*, 321–335.
- (3) Ulman, A. *An Introduction to Ultrathin Organic Films*; Academic Press: San Diego, 1991.
- (4) Dubois, L. H.; Nuzzo, R. G. *Annu. Rev. Phys. Chem.* **1992**, *43*, 437–463.
- (5) Ulman, A. *Chem. Rev.* **1996**, *96*, 1533–1554.
- (6) Finklea, H. O. in: *Electroanalytical Chemistry*; Marcel Dekker: New York, 1996; Vol. 19, pp 105–335.
- (7) Wink, T.; van Zuilen, A.; Bult, A.; van Bennekom, W. P. *Analyst* **1997**, *122*, R43–R50.
- (8) Laibinis, P. E.; Nuzzo, R. G.; Whitesides, G. M. *J. Phys. Chem.* **1992**, *96*, 5097–5105.
- (9) Joyce, S. A.; Thomas, R. C.; Houston, J. E.; Michalske, T. A.; Crooks, R. M. *Phys. Rev. Lett.* **1992**, *68*, 2790–2793.
- (10) Thoden van Velzen, E. U.; Engbersen, J. F. J.; de Lange, P. J.; Mahy, J. W. G.; Reinhoudt, D. N. *J. Am. Chem. Soc.* **1995**, *117*, 6853–6862.
- (11) Chailapakul, O.; Sun, L.; Xu, C.; Crooks, R. M. *J. Am. Chem. Soc.* **1993**, *115*, 12459–12467.
- (12) Erdelen, C.; Häussling, L.; Naumann, R.; Ringsdorf, H.; Wolf, H.; Yang, J.; Liley, M.; Spinke, J.; Knoll, W. *Langmuir* **1994**, *10*, 1246–1250.
- (13) Laibinis, P. E.; Whitesides, G. M. *J. Am. Chem. Soc.* **1992**, *114*, 9022–9028.
- (14) Laibinis, P. E.; Whitesides, G. M.; Allara, D. L.; Tao, Y.; Parikh, A. N.; Nuzzo, R. G. *J. Am. Chem. Soc.* **1991**, *113*, 7152–7167.
- (15) Edinger, K.; Göhlhäuser, A.; Demota, K.; Wöll, C.; Grunze, M. *Langmuir* **1993**, *9*, 4–8.
- (16) Poirier, G. E.; Tarlov, M. J.; Rushmeier, H. E. *Langmuir* **1994**, *10*, 3383–3386.
- (17) Delamarche, E.; Michel, B.; Gerber, C.; Anselmetti, D.; Güntherodt, H.; Wolf, H.; Ringsdorf, H. *Langmuir* **1994**, *10*, 2869–2871.
- (18) Camillone, N.; Chidsey, C. E. D.; Eisenberger, P.; Fenter, P.; Li, J.; Liang, K. S.; Liu, G.; Scoles, G. *J. Chem. Phys.* **1993**, *99*, 744–747.
- (19) Fenter, P.; Eberhardt, A.; Eisenberger, P. *Science* **1994**, *266*, 1216–1218.
- (20) Yeganeh, M. S.; Dougal, S. M.; Polizzotti, R. S. *Phys. Rev. Lett.* **1995**, *74*, 1811–1814.
- (21) Brückner, M.; Heinz, B.; Morgner, H. *Surf. Sci.* **1994**, *319*, 370–380.
- (22) Alves, C. A.; Smith, E. L.; Porter, M. D. *J. Am. Chem. Soc.* **1992**, *114*, 1222–1227.
- (23) Hähner, G.; Wöll, Ch.; Buck, M.; Grunze, M. *Langmuir* **1993**, *9*, 1955–1958.
- (24) Truong, K. D.; Rowntree, P. A. *Prog. Surf. Sci.* **1995**, *50*, 207–216.
- (25) Dannenberger, O.; Weiss, K.; Himmel, H.; Jäger, B.; Buck, M.; Wöll, C. *Thin Solid Films* **1997**, *307*, 183–191.
- (26) The kinetics of adsorption from the gas phase has been studied much less. (a) Thomas, R. C.; Sun, L.; Crooks, R. M.; Ricco, A. J. *Langmuir*, **1991**, *7*, 620–622. The mechanism for the vapor phase adsorption has recently been solved: (b) Poirier, G. E.; Pylant, E. D. *Science* **1996**, *272*, 1145–1148.
- (27) Buck, M.; Eisert, F.; Fischer, J.; Grunze, M.; Träger, F. *Appl. Phys. A* **1991**, *53*, 552–556.
- (28) Eisert, F. Ph.D. Thesis, University of Heidelberg, 1993.
- (29) Kim, Y.; McCarley, R. L.; Bard, A. J. *Langmuir* **1993**, *9*, 1941–1944.
- (30) Biebuyck, H. A.; Bain, C. D.; Whitesides, G. M. *Langmuir* **1994**, *10*, 1825–1831.
- (31) Shimazu, K.; Yagi, I.; Sato, Y.; Uosaki, K. *Langmuir* **1992**, *8*, 1385–1387.
- (32) Schneider, T. W.; Buttry, D. A. *J. Am. Chem. Soc.* **1993**, *115*, 12391–12397.
- (33) Pan, W.; Durning, C. J.; Turro, N. J. *Langmuir* **1996**, *12*, 4469–4473.
- (34) Karpovich, D. S.; Blanchard, G. J. *Langmuir* **1994**, *10*, 3315–3322.
- (35) Schlenoff, J. B.; Dharia, J. R.; Xu, H.; Weng, L.; Li, M. *Macromolecules* **1995**, *28*, 4290–4295.
- (36) Fruböse, C.; Doblhofer, K. *J. Chem. Soc., Faraday Trans.* **1995**, *91*, 1949–1953.
- (37) DeBono, R. F.; Loucks, G. D.; Manna, D. D.; Krull, U. J. *Can. J. Chem.* **1996**, *74*, 677–688.
- (38) Peterlinz, K. A.; Georgiadis, R. *Langmuir* **1996**, *12*, 4731–4740.
- (39) Bensebaa, F.; Voicu, R.; Huron, L.; Ellis, T. H.; Kruus, E. *Langmuir* **1997**, *13*, 5335–5340.
- (40) Perez, J.; Weiner, B. R. *Appl. Surf. Sci.* **1992**, *62*, 281–285.
- (41) Dannenberger, O. Ph.D. Thesis, University of Heidelberg, 1996, and Shaker Verlag: Aachen, 1997; ISBN 3-8265-2065-3.
- (42) Dannenberger, O. Diploma thesis, University of Heidelberg, 1993.
- (43) Richmond, G. L.; Robinson, J. M.; Shannon, V. L. *Prog. Surf. Sci.* **1988**, *28*, 1–70.
- (44) Shen, Y. R. *Nature* **1989**, *337*, 519–525.
- (45) Hall, R. B.; Russell, J. N.; Miragliotta, J.; Rabinowitz, P. R. *Chemistry and Physics of Solid Surfaces*; Springer Series in Surface Science, Vol. 28; Springer: Berlin, 1990; pp 87–131.
- (46) Corn, R. M.; Higgins, D. A. *Chem. Rev.* **1994**, *94*, 107–125.
- (47) Eisenthal, K. B. *Chem. Rev.* **1996**, *96*, 1343–1360.
- (48) Buck, M.; Grunze, M.; Eisert, F.; Fischer, J.; Träger, F. *J. Vac. Sci. Technol. A* **1992**, *10*, 926–929.
- (49) Chemla, D. S.; Zyss, J., Eds. *Nonlinear Optical Properties of Organic Molecules and Crystals*; Academic Press: New York, 1987; Vol. 1.
- (50) Buck, M.; Eisert, F.; Grunze, M.; Träger, F. *Appl. Phys. A* **1995**, *60*, 1–12.
- (51) For details of phase sensitive measurements see also: (a) Zhu, X. D.; Daum, W.; Xiao, X.; Chin, R.; Shen, Y. R. *Phys. Rev. B* **1991**, *43*, 11571–11580. (b) Berkovic, G.; Shvartsberg, E. *Appl. Phys. B* **1991**, *53*, 333–338. (c) Schwarzberg, E.; Berkovic, G.; Marowsky, G. *Appl. Phys. A* **1994**, *59*, 631–637.
- (52) Shen, Y. R. *The Principles of Nonlinear Optics*; Wiley: New York, 1984.
- (53) Tamada, K.; Hara, M.; Sasabe, H.; Knoll, W. *Langmuir* **1997**, *13*, 1558–1566.
- (54) Xu, S.; Cruchon-Dupeyrat, J. N.; Garno, J. C.; Liu, G.; Jennings, G. K.; Yong, T.; Laibinis, P. E. *J. Chem. Phys.* **1998**, *108*, 5002–5012.
- (55) Langmuir, I. *J. Am. Chem. Soc.* **1918**, *40*, 1361–1403.
- (56) Schlenoff, J. B.; Li, M.; Ly, H. J. *Am. Chem. Soc.* **1995**, *117*, 12528–12536.
- (57) Crank, J. *The Mathematics of Diffusion*, 2nd ed.; Oxford University Press: Oxford, UK, 1994.
- (58) Spinke, J.; Liley, M.; Schmitt, F.; Guder, H.; Angermaier, L.; Knoll, W. *J. Chem. Phys.* **1993**, *99*, 7012–7019.
- (59) Yamada, R.; Uosaki, K. *Langmuir* **1998**, *14*, 855–861.
- (60) Kreuzer, H. J. *Surf. Sci.* **1995**, *344*, L1264–L1270.
- (61) Arumainayagam, C. R.; Stinnett, J. A.; McMaster, M. C.; Madix, R. J. *J. Chem. Phys.* **1991**, *95*, 5437–5443.
- (62) de Gennes, P. G. *J. Chem. Phys.* **1971**, *55*, 572–579.
- (63) Atkins, P. W. *Physical Chemistry*, 4th ed.; Oxford University Press: Oxford, UK, 1990.
- (64) Berger, R.; Delamarche, E.; Lang, H. P.; Gerber, C.; Gimzewski, J. K.; Meyer, E.; Güntherodt, H. J. *Science* **1997**, *276*, 2021–2024.
- (65) Schessler, H. M.; Karpovich, D. S.; Blanchard, G. J. *J. Am. Chem. Soc.* **1996**, *118*, 9645–9651.
- (66) Himmelhaus, M.; Eisert, F.; Buck, M.; Grunze, M., manuscript in preparation.
- (67) Dannenberger, O.; Wolff, J. J.; Buck, M. *Langmuir* **1998**, *14*, 4679–4682.
- (68) Poirier, G. E. *Chem. Rev.* **1997**, *97*, 1117–1127.
- (69) Camillone, N.; Leung, T. Y. B.; Schwartz, P.; Eisenberger, P.; Scoles, G. *Langmuir* **1996**, *12*, 2737–2746.
- (70) Balzer, F.; Gerlach, R.; Polanski, G.; Rubahn, H. *Chem. Phys. Lett.* **1997**, *274*, 145–151.
- (71) Edinger, K.; Grunze, M.; Wöll, C. *Ber. Bunsen-Ges. Phys. Chem.* **1997**, *101*, 1811–1815.
- (72) Xia, T. X.; Landmann, U. *Science* **1993**, *261*, 1310–1312.
- (73) Jung, C.; Dannenberger, O.; Yue, X.; Buck, M.; Grunze, M. *Langmuir* **1998**, *14*, 1103–1107.
- (74) Dannenberger, O., unpublished results. This also explains the differences in the rate constant for thiol adsorption from ethanol between earlier studies and the present one. In the present experiments, substrates freshly evaporated and stored under inert gas atmosphere were used whereas no special storage was applied in the former experiments.^{27,48} Nevertheless, the adsorption mechanism remains unchanged.
- (75) unpublished.